Supercapacitors-based Power Supply for ASDEX Upgrade Toroidal Field Coils

A. Magnanimo[a,]*, M. Teschke[a], G. Griepentrog[b], the ASDEX Upgrade Team[a]

[a] *Max-Planck-Institute for Plasma Physics, 85748 Garching, Germany*
[b] *Technical University of Darmstadt, 64283 Darmstadt, Germany*

ASDEX Upgrade (AUG) electrical power is provided with three Flywheel Generators (FGs) that are charged up before the start of each plasma pulse with 15 MW for 30 minutes. The stored energy is then used to satisfy the high power needs during the pulse of up to 400 MW. The biggest FG ('EZ2') in case of a major fault could not be replaced by any other FG of such size because no comparable devices are available on the free market. Therefore, the development of an alternative energy storage with high power and energy density and fully controllable output is planned. Supercapacitors (SCs) are well known for their high specific power. The combination of this technology and a proper power converter topology such as the Modular Multilevel Converter (MMC) represent a promising alternative to be explored to replace Tokamaks FGs. The MMC topology allows a discrete-leveled output voltage and, thanks to its high cells number, it can operate continuously even in case of fault of some cells, while a FG could not. In this paper the concept of a SCs-based power supply for AUG's Toroidal Field (TF) Coils is presented, highlighting the main advantages and challenges of this project.

Keywords: Supercapacitors, Converter, Modular, Power Supply.

1. Introduction

AUG's electrical power is provided with three FGs (fig.1): EZ2, the largest one, provides power to the TF coils, while EZ3 and EZ4 supply the poloidal magnets, the ohmic heating and the additional heating systems. EZ2 is composed of a motor drive, a flywheel and a generator: its motors takes 5.7 MW for 30 minutes from the 10 kV / 50 Hz public network via a drive converter and accelerates the flywheel up to about 1600 min⁻¹. The energy taken from the grid is first converted into kinetic energy and then used to satisfy the much higher power needs during a plasma pulse of up to 150 MW.
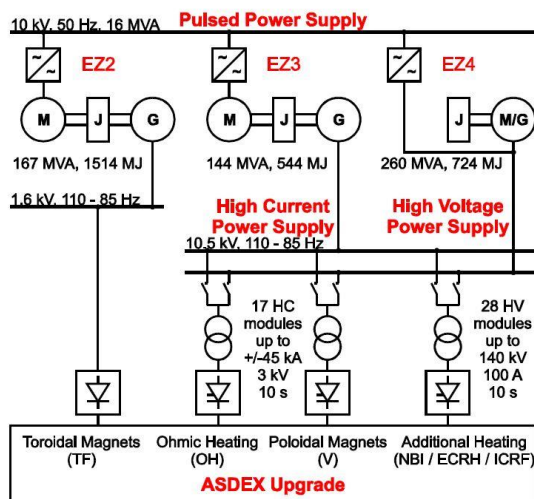

Fig.1: AUG power supply network: the 'EZ2' FG supplies the TF coils [1].

The main concern with the generator EZ2 is that, in case of a major fault, it could not be replaced by any other FG of such size because no comparable devices are

available on the free market anymore. SCs are well known for their high power density, and they are similar to FGs in terms of energy density. Some SCs-based applications for Tokamaks coils high power requirements are already under development [2]. Fig.2 shows a comparison among SCs, FGs, common batteries and standard capacitors: SCs have a higher power density (up to 5-10kW/kg) than a Li-ion battery, but it has a significantly lower energy density [3]; due to their material composition and design structure SCs have also a lower Equivalent Series Resistance (ESR). These characteristics lead to higher efficiency, larger current charge and/or discharge capacity and lower heating losses. Thanks to their high power density, SCs have several potential applications, but they are mainly used for uninterruptible power systems (UPSs) and hybrid electric vehicles (HEVs) [4].
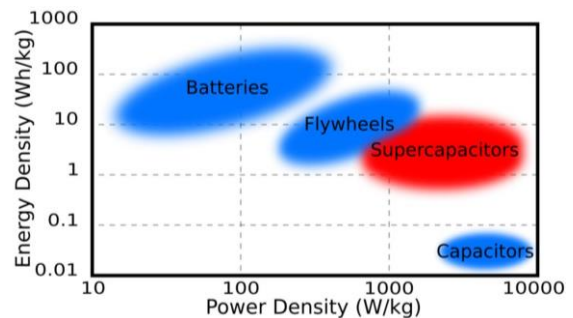

Fig.2: Comparison among SCs, FGs, common batteries and capacitors in terms of energy and power density [3].

SCs therefore represent a promising alternative to be explored to replace the FG EZ2. However, they cannot be directly connected to the coils and they need a suitable converter topology able to drive their output current in a controlled way. During AUG's pulses, indeed, in order to ensure a proper plasma confinement the temporal toroidal magnetic field ripple must not

---

exceed a fixed value. Since it strictly depends on the toroidal field coils current ripple (defined in section 4), a proper converter able to control that current must be adopted.

2. The MMC Topology for AUG's TF Coils

The AUG's TF coils are actually supplied only by the FG EZ2 and a diode converter. The 16 TF coils (in series connection) represent an inductance of 120 mH and a resistance of 14 mΩ, since they are not superconductive. Fig.3 shows the main electrical requirement of such coils during a typical plasma pulse. The current is first ramped-up, than kept smooth and constant during the flat-top phase and finally ramped-down at the end of the pulse (top row in fig.3). The TF coils impedance is almost perfectly constant and decoupled from the other loads of the tokamak. The ramp-up and ramp-down are not optimal, because the current control is directly realized by modifying the magnetic excitation of the FG, which has a large time constant (approximately 500 ms). The voltage needed during the ramp-up phase is higher (2.6 kV) than during the flat-top phase with approximately 800 V (to cover ohmic losses) for a current of approximately 54 kA to provide a typical TF magnetic field of 2.5 T in the tokamak vessel. The energy need during flat-top phase is in the range of 0.5 GJ. A detailed description of AUG's actual power supply can be found in [1].
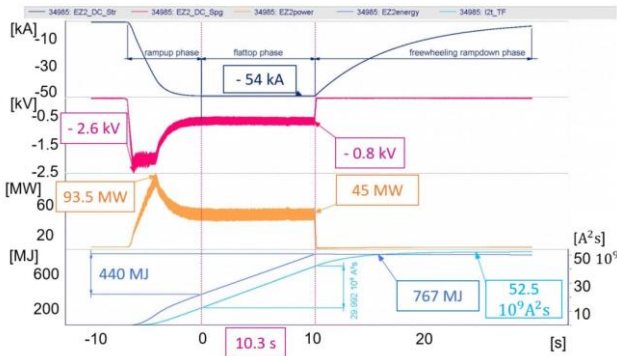

Fig.3: AUG's TF coils electrical requirements during a typical experiment. From top to bottom rows: current, voltage, power, energy consumption and $i^2 t$;

The MMC topology (fig.4) is mainly used for High-Voltage DC Transmission (HVDC), medium voltage application and flexible AC transmission systems. The standard converter topology for three phase applications consists of six arms, each of which contains a series connection of n cells and an inductor L. Each cell (or switching module) contains a half-bridge of two Insulated Gate Bipolar Transistors (IGBTs) and a capacitor (C_{SM}). The capacitor C_{SM} is loaded with the voltage v_C that is influenced by the phase current which flows through the three-phase load (U, V, W). Each switching module (SM) can be toggled between two different states (see fig.5):

- ON-state: the current flows through the upper switch ($v_{SM} = v_C$);

- OFF-state: the current flows through the lower switch ($v_{SM} = 0$).

If r cells of n are in the ON-state (with $0 \leq r \leq n$), the sum voltage of these r capacitor voltages is generated over the respective phase [5]. The main advantages of this converter topology are summarized below:

- Modular structure with identical modules;
- Scalable voltage;
- Possibility to substitute failed modules;
- Stored energy is distributed among the submodules and can be therefore better handled in case of a failure;
- Simple mechanical construction.

The challenge of realizing this topology comes from the high number of semiconductors and gate units, which leads to a complex controller.
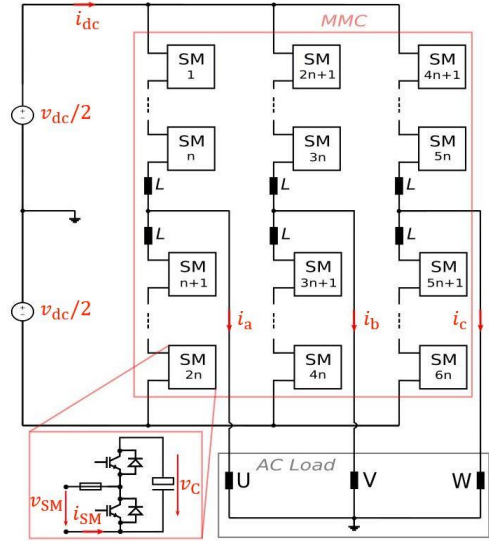

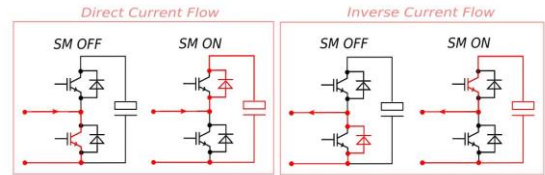Fig.4: Conventional MMC for three-phase AC loads;

Fig.5: SM with half bridges: possible states;

A reduced version of a MMC topology suitable to fulfill the needs to replace EZ2 is shown in fig.6. It consists of a single arm (since the TF coils represent a single-phase load) of the MMC topology where C_{SM} is replaced by a SCs module with the option to increase the total output current thanks to the parallel operation of multiple SMs. The charger is composed by a three-phase diode bridge that rectifies voltage and current taken from the 10 kV / 50 Hz network (via step-down transformer to be defined) and charges up the SCs modules by the help of the SMs switches. The charging process is discussed in detail in the next section.

The communication among SMs will be based on the EtherCAT protocol [6]. Every row (where a row is defined by m parallel and synchronized SMs, see fig.7) has a so called 'row controller' and m cell controllers: the row controller communicates only with the first and the last SMs of its row (ring topology); the information (gate signals, voltage, current, temperature and SMs

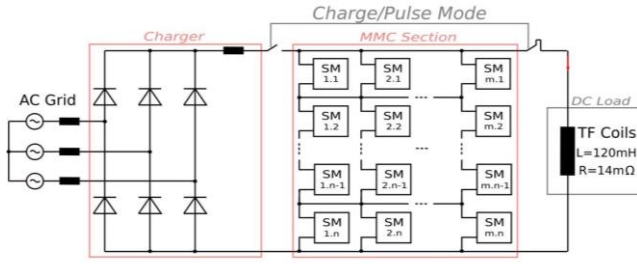status information) is than exchanged among adjacent cell controllers.

Fig.6: Proposed topology for AUG's TF coils;

The 'Distributed clocks method' ensure synchronization of the SMs: every cell controller has its own clock which is synchronized with a reference clock (usually the one of the first SM of the row); the jitter among cell controllers is calculated and compensated during the network initialization. A second communication path (equal to the first one but opposite in direction) guarantees redundancy in case of failure of one SM [7]. SMs failures are locally managed by the cell controllers (the row controller only receive information about their status): thanks to an additional switch (represented as local virtual fuses in the fig. 7 for simplicity, but the type of switch that will be adopted has still not be defined), its cell controller will isolate such SM without affecting the row's operation and the its current, thanks to the arm interconnections, will flow through the other *m-1* SMs. The master controller communicates via a master communication bus with the *n* row controllers from which receives voltage, current and status information of the rows and it finally implements the current control, choosing the rows to connect/disconnect depending on their voltage levels. This approach is optimal in terms of scalability since the required power electronics, once developed, can be duplicated, no matter how large the energy demand and therefore the total matrix is.
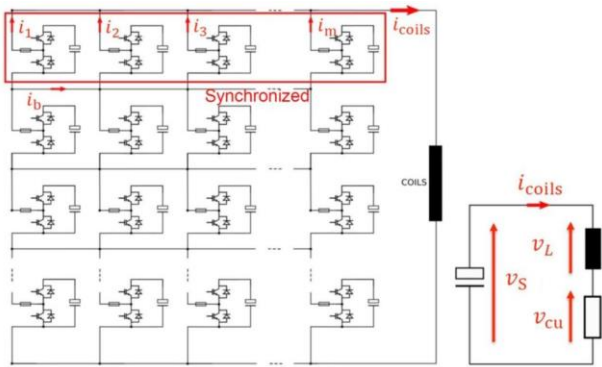

Fig.7: Pulse phase configuration (left) and its equivalent circuit (right);

The SC module chosen for this project is the 'BMOD0071 P130 B04' from Maxwell Technologies, composed of 48 2.7 V SCs connected in series for a total voltage of 130 V, a capacitance of 71 F, a peak current of 2 kA and a ESR of 17 mΩ. With the proposed topology, in order to supply all AUG's TF coils, 23 rows in series (*n*) and 61 parallel arms (*m*) would be required to reach the 3 kV (including 400 V of safety margin) and

the 54 kA needed during a pulse, which means about 1400 total SCs modules. Their weight would reach almost 60 tons (counting only SCs modules, about 42 kg/module). Considering that the EZ2's flywheel weights 220 tons, the gain in terms of weight would be relevant.

3. The Charging Process

The charging process is divided in two sub-phases: the pre-charging phase (PCP) and the boost charging phase (BCP). The PCP is realized thanks to a low power step-down converter, used as pre-charger (see fig.8): it slowly charges up simultaneously SCs modules belonging to the same rows exploiting SMs switches; the rows are indeed connected one by one to the pre-charger, reaching the voltage required by the BCP. During the BCP (see fig.9), SCs modules are charged up at their full voltage with a boost converter-based charger realized by the help of the power stage IGBTs to simplify scalability. During this phase an inductor (which also limits the di/dt of the charging current) first stores energy and then charges SCs with such energy. In order to transfer inductor's stored energy into SCs, the di_L/dt must be negative. Since the voltage across the inductor is:

$$v_L = v_i - v_0. \qquad (1)$$

v_0 - defined as the output voltage of the charger - must be higher than the input voltage v_i. For this reason the PCP is required.
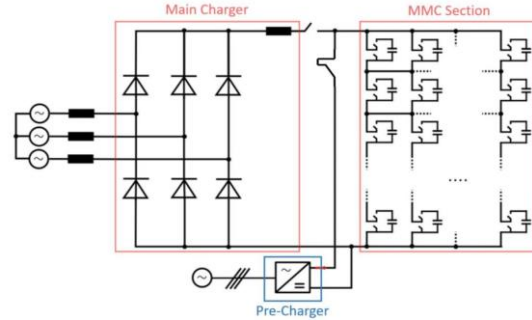

Fig.8: A pre-charger is used for charging the SCs at the voltage level required by the BCP;
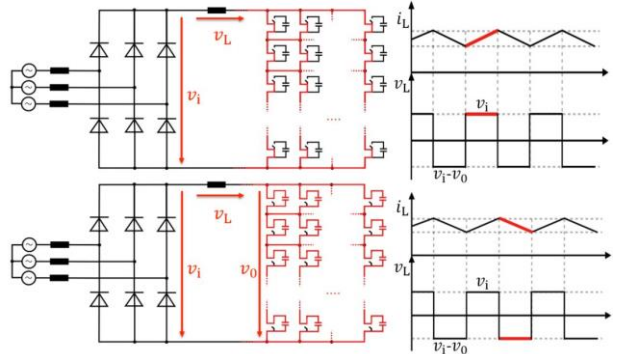

Fig.9: First (top) and second (bot) sub-phases of the BCP;

Some simulations have been performed with PLECS for a better understanding of the charging process seen from the single SCs module (see fig.10).
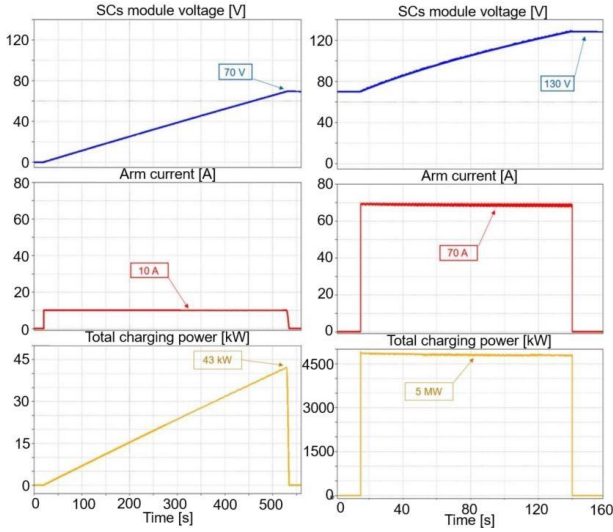
Fig.10: SC module Voltage, arm current and charging power during the PCP (left) and BCP (right);

Considering the voltage and current chosen as constraints (10 A to avoid excessive SCs stress and 70 V required by the BCP) and the number of parallel modules of the topology a pre-charger of 43 kW would require about 8 min to charge up at 70 V each row of SCs modules with a total current of 610 A (61 parallel modules). The constraints for the BCP are the available power and the charging time: the first one is limited at 5 MW (maximum available power from the AC grid) and the second one must be as low as possible; with a total charging current of 4.2 kA (70 A per arm) and an input voltage of 1.5 kV the charger would require about 120 s to charge at the full voltage the SCs modules, which fits the actual requirements of AUG's TF coils.

4. The Pulse Phase

Once the SCs are charged up at their full voltage, they are ready to power the coils with their stored energy. The charger circuit for this purpose can be disconnected from the SMs which are then connected only to the coils, as shown in fig.7. The topology during this phase can be represented with the equivalent circuit shown in the right-hand side of fig.7 where the TF coils are represented by a series RL circuit (v_L represent the voltage over the coils inductance while v_{cu} represent the voltage drop over their resistance) and the SMs matrix is represented by a variable voltage source (v_S) that assumes a different voltage level depending on the number of rows connected. During the ramp-up phase i_{coils} is raised at 54 kA as fast as possible (a faster ramp-up phase means less losses during such time frame), and to do so $v_S - v_{cu}$ must be maximized, which means that all the available rows of the matrix will be used to keep v_S as high as possible. The flat-top phase is the most crucial one; in this phase the current should be ideally constant at about 54 kA for about 10 s (depending on the requirements of the plasma pulse), but in reality the coils current presents a ripple (Δi) which must be kept below 0.1% of i_{coils}'s value. Δi is defined as:

$$\Delta i \approx \frac{v_S - v_{cu}}{L_{Coils}} \cdot t_{on/off} \qquad (2)$$

where t_{on} is the time during which $v_S - v_{cu}$ is positive (Δi positive) and t_{off} is the time during which $v_S - v_{cu}$ is negative (Δi negative). Fig.11 shows an ideal frame (v_{cu} variation due to Δi as well as SCs voltage loss have been neglected) of the flat-top phase highlighting the values assumed by v_S during t_{on} and t_{off}. From the circuit in fig.7 therefore it is clear that for $v_S > v_{cu}$, i_{coils} increases, while for $v_S < v_{cu}$ it decreases with a slope that depends on $|v_S - v_{cu}|$, which is then minimized. Minimizing $|v_S - v_{cu}|$ means that v_S assumes the closest available values to v_{cu} (shown in fig.11, where Δv depends on the voltage level of the row added/removed). Increasing the switching frequency of IGBTs would also limit Δi ($t_{on/off}$ would decrease), but it would increase the switching losses of the power electronics and reduce the lifetime of the SCs as well. For this reason it will be kept as low as possible and the 'first choice' considered to lower the current ripple is the voltage.
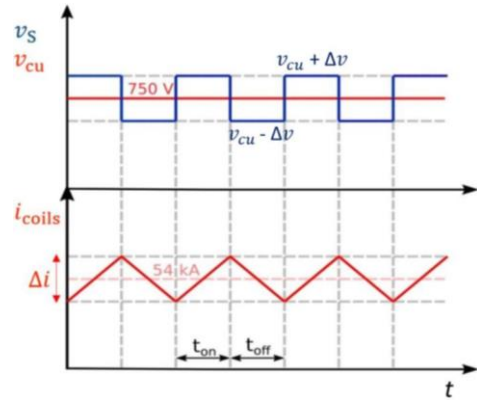

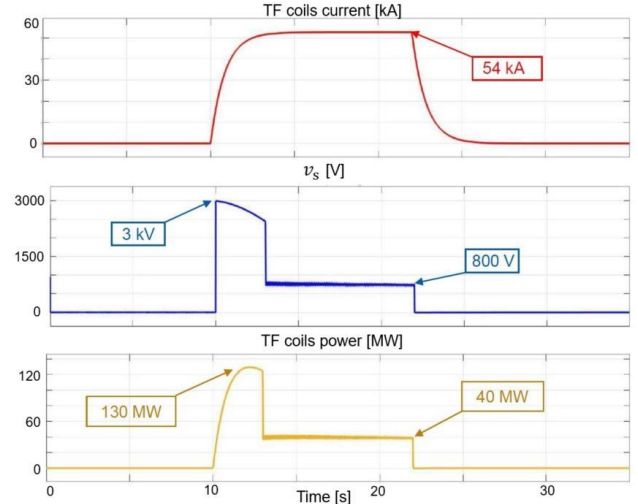*Fig.11: v_S, v_{cu} and i_{coils} during a frame of the flat-top phase;*

Fig.12: i_{coils} (top), v_S (mid) and TF coils power (bottom) during a standard 10 s pulse;

During the ramp-down phase, finally, the SMs are shorted and the inductive energy of the TF coils is dissipated in their internal resistance. The i_{coils} variation is negative during this phase and it becomes zero once all the energy stored into the coils is dissipated. Such energy could in principle be recovered, and used to recharge of a few V the SCs, but in this case the switching module would have to be IGBT full-bridges instead of a half-bridges [5], which would double conduction losses of the power electronics, because in

that case two IGBTs would continuously conduct while with the half-bridge only one is conducting.
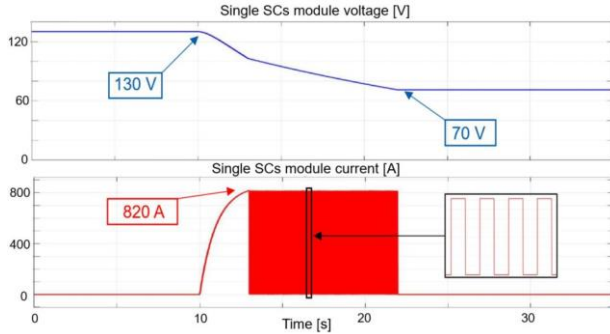

Fig.13: Single SCs module voltage (top) and current (bot) during a standard 10 s pulse;

Some simulations have been performed for the pulse phase as well. Fig.12 shows i_{coils}, v_S, and the required power during a standard 10s pulse, while fig. 13 shows voltage and current curves of the single SCs module during a plasma pulse. During the flat-top phase, the SCs must only cover the copper losses and then they operate in a switched operation. From the coils side a $f_{sw} = 4$ Hz is enough to keep the current ripple below 50 A, but in order to keep SCs voltages balanced they will operate at a higher frequency. The current flowing across a SCs module indeed is:

$$i_{SC} = C_{SC} \cdot \frac{dv_{SC}}{dt_{on}} \qquad (3)$$

where $i_{SC} = 820$ A, $C_{SC} = 71$ F and dv_{SC}/dt_{on} is the voltage variation during the ON time t_{on}. From the equation above, setting dv_{SC} at 0.1 V (it has been decided to start from a conservative value that can be later increased) a switching frequency of about 100 Hz ($1/t_{on}$) has been estimated. Assuming a duty cycle of 50% (D), SCs losses can also be estimated as:

$$P_{SC,loss} = D \cdot ESR \cdot i_{SC}^2 = 6 \text{ kW} \qquad (4)$$

referred to a single SCs module. This means that the total power dissipated within SCs internal resistance is than 8 MW.

5. Conclusion

This paper shows the concept of a SCs-based power supply that could replace in future EZ2 AUG's FG, highlighting advantages and challenges of such project. This alternative solution is under development, indeed, to be ready for eventual permanent failure of the actual machine. A Modular Multilevel Converter (MMC) topology has been adapted to drive SCs energy into tokamak's coils since the high number of cells of this structure allows more flexibility than a FG and in case of fault of some modules the converter can continue its operation, while a FG could not. The development of the master, row and SM controllers has been started to realize a small-scale demonstrator: the full controlled operation of a single SM will be first demonstrated; furthermore a MMC arm composed by at least two SMs will be realized and finally it will be duplicated to demonstrate parallel operation, that would indeed fulfil

the requirements for an 'infinite' scalability of this project.

References

[1] C.-P. Kaesemann, "Pulsed Power Supply System of the ASDEX Upgrade Tokamak Reseach Facility", *2015 IEEE 15th International Conference on Environment and Electrical Engineering*, July 2015. https://doi.org/10.1109/EEEIC.2015.7165545

[2] A. Lampasi, R. Romano, A. Cocchi and P. Zito, "Poloidal Power Supply System of the Divertor Tokamak Test (DTT) Facility," *2020 IEEE 20th Mediterranean Electrotechnical Conference (MELECON),* Palermo, Italy, 2020, pp. 634-639. *https://doi.org/10.1109/MELECON48756.2020.9140640*

[3] I. Ciocan, C. Farcas, A. Grama, A. Tulbure, "An Improved Method for the Electrical Parameters Identification of a Simplified PSpice Supercapacitor Model", *2016 IEEE 22nd International Symposium for Design and Technology in Electronic Packaging*, pp. 171-174, 2016. https://doi.org/10.1109/SIITME.2016.7777270

[4] L. Shi and M. L. Crow, "Comparison of Ultracapacitor Electric Circuit Models", *2008 IEEE Power and Energy Society General Meeting - Conversion and Delivery of Electrical Energy in the 21st Century,* July 2008. https://doi.org/10.1109/PES.2008.4596576

[5] U. K. Kalla, A. Verna, B. Singh and K. Joshi, "A Controller for Cascaded H-Bridge Multilevel Inverter", *2016 IEEE 7th Power India International Conference (PIICON),* November 2016. https://doi.org/10.1109/POWERI.2016.8077312

[6] M. Rostan, J. E. Stubbs and D. Dzilno, "EtherCAT enabled advanced control architecture," *2010 IEEE/SEMI Advanced Semiconductor Manufacturing Conference (ASMC)*, San Francisco, CA, 2010, pp. 39-44. https://doi.org/10.1109/ASMC.2010.5551414

[7] P. Dan Burlacu, L. Mathe, M. Rejas, H. Pereira, A. Sangwongwanich and R. Teodorescu, "Implementation of fault tolerant control for modular multilevel converter using EtherCAT communication," *2015 IEEE International Conference on Industrial Technology (ICIT)*, Seville, 2015, pp. 3064-3071. https://doi.org/10.1109/ICIT.2015.7125551